P H Y S I C A L   R E V I E W   L E T T E R S

Geometry and Regularity of Moving Punctures

Mark Hannam,[1] Sascha Husa,[1] Denis Pollney,[2] Bernd Brügmann,[1] and Niall Ó Murchadha[3]

[1]*Theoretical Physics Institute, University of Jena, 07743 Jena, Germany*
[2]*Max-Planck-Institut für Gravitationsphysik, Albert-Einstein-Institut, Am Mühlenberg 1, 14476 Golm, Germany*
[3]*Physics Department, University College Cork, Ireland*

Significant advances in numerical simulations of black-hole binaries have recently been achieved using the puncture method. We examine how and why this method works by evolving a single black hole. The coordinate singularity and hence the geometry at the puncture are found to change during evolution, from representing an asymptotically flat end to being a cylinder. We construct an analytic solution for the stationary state of a black hole in spherical symmetry that matches the numerical result and demonstrates that the evolution is not dominated by artefacts at the puncture but indeed finds the analytical result.

Recent breakthroughs in numerical relativity have made it possible to simulate the evolution of black-hole binaries through several orbits, inspiral, merger, and ringdown [1–4]. It is now possible, after over forty years of research, to study black-hole mergers in full general relativity and to calculate the resulting gravitational-radiation waveforms. These advances represent a major step forward for all of black-hole and gravitational-wave astronomy and astrophysics.

Although these methods have met with spectacular success, it is not yet clear how and why they work. In this Letter we focus on the most popular method, called "moving punctures" [2,3], and use simple geometrical considerations to address this question. In the moving-puncture method the black holes are conveniently described in the initial data in coordinates that do not reach the black holes' physical singularities; as the coordinates approach each singularity they instead follow a wormhole through to another copy of the asymptotically flat exterior spacetime. These extra copies are compactified so that their infinities are represented by single points on a numerical grid, which are called "punctures" [5,6]. In this construction, the wormhole topology is captured by a single function, a conformal factor ψ, which diverges at each puncture. Early "fixed puncture" evolutions [7,8] factored the singularity into an analytically prescribed conformal factor, and the gauge conditions prohibited the punctures from moving across the grid. The moving puncture approach manages to evolve the full conformal factor, ψ, and the punctures are allowed to move. This seemingly minor modification proved to be the last piece of the black-hole binary puzzle, and it has made long-term stable simulations routine for many research groups.

However, the dynamical behavior of the punctures in this method is entirely unknown. Do they continue to represent compactified infinities? Does the evolution reach a final, stationary state, or do gauge dynamics persist? And, crucially, does the method accurately describe the spacetime, or does it rely on numerical errors near an underresolved puncture, implying that it may fail when probed at

higher resolutions or for longer evolutions? Finally, why do our coordinate conditions accurately reproduce angular velocities as would be measured in an asymptotic rest frame (see, e.g., [9])?

In this Letter we address these questions in three stages. First, we argue that the evolution of the punctures can be split approximately into advection across the hypersurface plus a gauge that locally produces black holes in a stationary state. Second, we assume existence of a stationary solution and show that a local expansion for a Schwarzschild puncture matches the numerical data. And third, we explicitly construct stationary slices for Schwarzschild and discuss their global geometry, to which the numerical evolution asymptotes.

Most significantly, we find that the puncture changes character: the slice no longer approaches the other asymptotically flat end, but ends on a cylinder of finite areal radius. This suggests an elegant new way to represent black holes, with asymptotically cylindrical data.

Let r be the distance to one of the punctures. Internal asymptotically flat ends are characterized by 3-metrics of the form $g_{ij} = \psi^4 \tilde{g}_{ij}$, where $\tilde{g}_{ij}$ is finite and the conformal factor ψ diverges as $\psi \sim 1/r$. The method of [2] introduces a regular conformal factor $\chi = \psi^{-4}$ while [3] uses $\phi = \log \psi$. Ignoring the $\log r$ singularity, standard finite-differencing is used near the punctures. The evolution method is based on the Baumgarte-Shapiro-Shibata-Nakamura (BSSN) formulation [10,11]. For the lapse we consider "1 + log" slicing, $(\partial_t - \beta^i \partial_i)\alpha = -2\alpha K$, and for the shift the "Gamma-freezing" condition, $\partial_t^2 \beta^i = \frac{3}{4}\partial_t \tilde{\Gamma}^i - \eta \partial_t \beta^i$ [2,12–14].

Puncture evolutions use the standard $3 + 1$ decomposition, and the equations can be brought into the form $(\partial_t - \mathcal{L}_\beta)u = F$, where u is a state vector and F a source term independent of the shift. In this context we do not have to consider the BSSN variable $\tilde{\Gamma}^i$ since it is derived from $\tilde{g}_{ij}$. Of special importance is the motion of the puncture itself, which is marked by a $\log r$ pole in ϕ or equivalently a zero in χ [2], which are advected by the shift like all other

variables. As noted in [2,3,8,12], since the shift can describe arbitrary coordinate motion, any shift vector that does not vanish at the puncture can generate motion of the puncture.

The Gamma-freezing shift manages two feats: stabilizing the black holes against slice stretching and moving the punctures. Considering that in actual runs those two effects appear to happen independently of each other, we propose that the shift can be split as $\beta^i = \beta^i_{\text{adv}} + \beta^i_{\text{sls}}$, where β^i_{sls} counters slice stretching and β^i_{adv} is responsible for puncture motion. If we have *exact* stationarity, then $(\partial_t - \mathcal{L}_{\beta_{\text{adv}}})u = 0$, $\mathcal{L}_{\beta_{\text{sls}}}u + F = 0$. Note that in the early phase of a binary inspiral simulation the vector $(\frac{\partial}{\partial t})^a$ should be an approximate helical Killing vector, up to a rigid rotation. We can choose either corotation, or vanishing rotation at infinity, which would imply that the punctures' coordinate speeds equal their physical speeds as seen from infinity.

In general, this shift decomposition will hold only approximately, but it should be an excellent approximation in the immediate vicinity of the punctures. Furthermore, if the shift is regular at a puncture with a leading constant plus higher order terms, $\beta^i = b^i_0 + O(r)$, $\beta^i_{\text{adv}}|_{r=0} = b^i_0$, $\beta^i_{\text{sls}}|_{r=0} = 0$, then we obtain trivial advection of the puncture without further approximation, i.e., $u = u(x + b_0 t)$, since $\mathcal{L}_{b_0}u = b^i_0 \partial_i u$.

We conclude that, assuming approximate stationarity, the question of numerical stability of the moving-puncture process can be approached by splitting it into a standard advection problem and a stability analysis of a stationary puncture solution. The main open issue is whether there exists a regular stationary solution for a single puncture that the method can find. Since the key novel features of this stationary solution already occur for a nonmoving spherically symmetric puncture (computed with the moving-puncture method), we focus on this case here and leave the general case to future work.

Consider initial data for a single puncture with mass M at $t = 0$, with $\alpha = 1$, $\beta^i = 0$, $\tilde{g}_{ij} = \delta_{ij}$, $\tilde{A}_{ij} = 0$, $K = 0$, and $\phi_0 = \log(1 + \frac{M}{2r})$. When inserted into the BSSN and gauge equations, the data evolve and develop certain powers of r at the puncture [12]. If a regular stationary state is reached, then all variables should possess power series expansions at $r = 0$ that satisfy $\mathcal{L}_{\beta_{\text{sls}}}u + F = 0$. We make the following ansatz for the single, nonmoving-puncture case in spherical symmetry:

$$\psi^{-2} = e^{-2\phi} = p_1 r + p_2 r^2 + O(r^3), \qquad (1)$$

$$\tilde{g}_{ij} = \delta_{ij} + O(r^2), \qquad (2)$$

$$\tilde{A}_{ij} = (A_0 + A_1 r)(\delta_{ij} - 3n_i n_j) + O(r^2), \qquad (3)$$

$$K = K_0 + K_1 r + O(r^2), \qquad (4)$$

$$\alpha = a_0 + a_1 r + O(r^2), \qquad (5)$$

$$\beta^i = (b_1 r + b_2 r^2)n^i + O(r^3). \qquad (6)$$

Here $r = (x^2 + y^2 + z^2)^{1/2}$ is the coordinate radius of

quasi-isotropic Cartesian coordinates (x, y, z). Note that r is continuous but not differentiable, the radial vector $n^i = x^i/r$ is discontinuous at $r = 0$, and $\partial_i O(r^0) = O(r^{-1})$. The evolution equations and the constraints result in 8 independent equations for the 10 coefficients (p_1, p_2, A_0, A_1, K_0, K_1, a_0, a_1, b_1, b_2), with M and η free parameters. The Gamma-freezing shift condition does not give an additional condition for a stationary solution. A first result is that $a_1 \neq 0$ and $K_0 \neq 0$ are required for nontrivial stationarity; a more regular solution is not consistent with the equations. For consistency $a_0 = 0$, that is, the lapse has collapsed at the puncture. Further simple relations are $b_1 = 2K_0$ and $b_2 = -3A_0 a_1$ from the evolution equations for the lapse and the metric.

Therefore, assuming existence of a stationary solution with some minimal regularity at the puncture implies specific predictions for kinks and discontinuities in our variables. We now compare the ansatz to numerical results for a Schwarzschild puncture evolved to $t = 50M$, at which time the data appear to have reached a stationary state to within a few percent in all variables. The runs were performed with the BAM code, using fixed-mesh refinement and fourth-order accurate finite-difference stencils [15]. For a central resolution of $M/128$ the run is well within the convergent regime. When zooming into the data at this resolution, Fig. 1, we do find the kinks and discontinuities consistent with the ansatz. Although closer inspection shows some numerical artefacts near the puncture (in particular, in $\tilde{A}_{ij}$ and the derivatives), they remain localized and comparatively small, and the numerical data are approximated well by the ansatz.

The most intriguing implication of the power series expansion is that the singularity in the conformal factor changes during evolution. With $a_0 = 0$,

$$\partial_t \phi = \beta^i \partial_i \phi + \frac{1}{6} \partial_i \beta^i + O(r) \simeq b_1 r \partial_r \phi + \frac{b_1}{2}. \qquad (7)$$

For the conformal factor of the initial data, we have $r \partial_r \phi_0 \simeq -1$, and $\partial_t \phi_0 \simeq -b_1/2$. With $b_1 \neq 0$ we must conclude that the evolution of the conformal factor will stop only when $r \partial_r \phi \simeq -1/2$. In other words,

$$\psi_0 = O(1/r) \quad \text{evolves into} \quad \psi = O(1/\sqrt{r}), \qquad (8)$$

which is built into (1). The puncture still marks a coordinate singularity, but since the areal radius of the sphere $r = 0$ is $R_0 = \lim_{r \to 0} r\psi^2 = 1/p_1$, the slice no longer reaches the other asymptotically flat end of the Brill-Lindquist wormhole, but ends at a finite areal radius, $R_0 \approx 1.3M$, with p_1 determined numerically. Figure 2 illustrates the evolution of a Schwarzschild black hole. We have plotted Schwarzschild R versus proper distance from the horizon. The initial slice connects two asymptotically flat regions, but during a $1 + \log/\Gamma$-driver evolution the numerical slice loses contact with the second asymptotically flat end. It eventually reaches a stationary state and terminates at $R \approx 1.3M$.
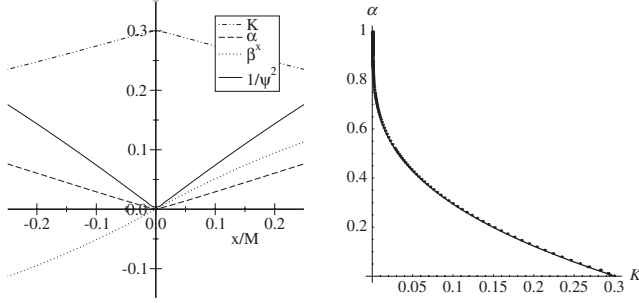
FIG. 1.   Numerical evolutions of a spherically symmetric puncture result in specific kinks at the puncture (left). The figure on the right represents a true numerical experiment. We compare two spherical slices by plotting α as a function of K. The dots are the data from the 3D numerical evolution; the solid line was obtained by independently integrating up Eq. (9). At the puncture, $\alpha \approx 0.0$ and $K \approx 0.3$.

We now show by explicit construction in the proper distance gauge (which is regular through the horizon) that such stationary slices exist globally. Stationary $1 +$ log slices of Schwarzschild are also considered in a different context in [16]. The proper distance coordinate is denoted as l, $\partial_l f = f'$, α is the Killing lapse, β the Killing radial shift component, and R the areal radius (the Schwarzschild radial coordinate). On any spherical slice through the Schwarzschild solution one finds $R' = \alpha$ and $\alpha^2 - \beta^2 = 1 - 2M/R$, and using these, the equation for the stationary $1 +$ log slices of Schwarzschild, $\beta\alpha' = 2\alpha K$, becomes (using, for example, [17])

$$R'' = \frac{2R'}{R} \frac{\frac{3M}{R} - 2 + 2R'^2}{\frac{2M}{R} - 1 + R'^2 - 2R'}. \tag{9}$$

It is clear that the right-hand side of (9) is singular whenever $2M/R - 1 + R'^2 - 2R' = 0$. It can also be shown that any solution of (9) that is suitably asymptotically flat, i.e., $R \approx l$, must pass through such a singular point. The only way of resolving this difficulty is for the numerator of (9) to simultaneously vanish at the "singular" point. We have two options: either (a) $R' = 0$ or (b) $3M/R - 2 + 2R'^2 = 0$. Let us discuss them separately. In the case (a), we have $R' = 0$, $R = 2M$. Therefore, the slice passes through the bifurcation sphere. This is the standard moment of time symmetry slice through the Schwarzschild solution, which obviously satisfies the stationary $1 +$ log equation because $\beta \equiv 0$ and $K \equiv 0$. In case (b), the case in which we are really interested, we can solve the pair of simultaneous equations to give $R' = \sqrt{10} - 3$, $R \approx 1.54M$. This solution corresponds to two slices in the Schwarzschild solution. These are mirror images of each other: one in the upper half plane, one in the lower. These slices do not continue into the left quadrant of the extended Schwarzschild solution. Rather they asymptote to a cylinder in the upper (lower) quadrant of fixed radius. This agrees with the numerical observation that the singularity in the conformal factor changes from $1/r$ to $1/\sqrt{r}$. These
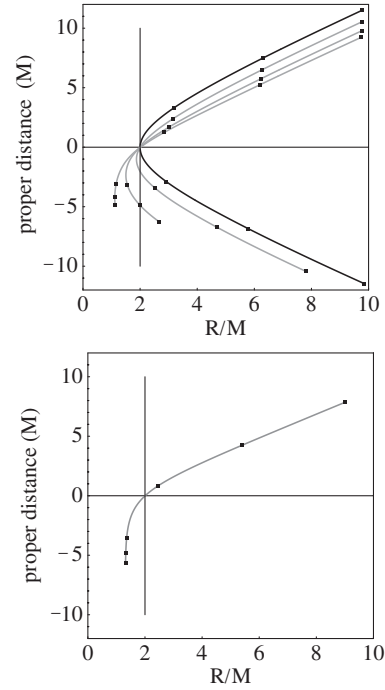

FIG. 2.   Schwarzschild coordinate R vs proper distance from the (outer) horizon. The upper panel shows the slices at $t = 0, 1, 2, 3M$, and the lower panel shows the slice at $t = 50M$. The final numerical slice terminates at $R \approx 1.3M$. The vertical line indicates the horizon at $R = 2M$, and the six points represent $x/M = 1/40, 1/20, 1/8, 2, 5, 8$ on each slice.

three are the only asymptotically regular solutions of the stationary $1 +$ log equation, up to isometries. It is easy to show that the actual slice exponentially approaches a cylinder of radius R_0, i.e., $R \approx R_0 + A\exp(Bl)$ as $l \to -\infty$, where

$$B = 2R_0^{-1}(3M - 2R_0)(2M - R_0)^{-1}.$$

The value of the lapse at the horizon, which can be used as a simple horizon-finding or merger-time criterion, evaluates to $\alpha(R = 2M) \approx 0.376$. It is also possible to produce an algebraic solution in terms of an implicit equation for α and R, determining $R_0 \approx 1.31241M$ from

$$3\sinh^{-1}(3) = \log\left[128\left(2 - \frac{R_0}{M}\right)\right] + 3\log\left(\frac{R_0}{M}\right) + \sqrt{10} - 3.$$

For comparison we have also studied harmonic and maximal slicing. With harmonic slicing (which can be generalized to the Kerr spacetime [18,19]), one again finds a moment of time symmetry slice and two mirror copies of a slice that puncture evolutions driven toward stationarity should approach. The slices hit the singularity at $R = 0$, K blows up as $R \to 0$, and at the horizon $\alpha(R = 2M) = 1/2$. Fixed-puncture evolutions have used $1 +$ log slicing without shift term. Stationary slices must then be maximal [20–22], of the "odd lapse" type, $\alpha^2 = 1 - \frac{2M}{R} + \frac{C^2}{R^4}$. For $C = 3\sqrt{3}M^2/4$ such slices will again approach a cylinder, of constant $R_0 = 3M/2$.

Discussion.—Moving-puncture evolutions of a Schwarzschild black hole approach a stationary slice that neither reaches an internal asymptotically flat end nor hits the physical singularity, as might be expected for a stationary slice with non-negative lapse [23]. Rather, the slice ends at a throat at finite Schwarzschild radius, but infinite proper distance from the apparent horizon. This changes the singularity structure of the ''puncture.'' It is still a puncture in that there is a coordinate singularity at a single point in the numerical coordinates, but it does not correspond to an asymptotically flat end. In the course of Schwarzschild evolutions we have found that the throat does collapse to the origin. Where one would have expected an inner and an outer horizon, we find only one zero in the norm of $(\frac{\partial}{\partial t})^a$, corresponding to the outer horizon. An under-resolved region does develop in the spacetime (it is the region between the throat and the interior spacelike infinity), but we are pushed out of causal contact with it. The throat itself has receded to infinite proper distance from the outer horizon. Matter fields or gravitational radiation will be trapped between the inner horizon and the throat, because unlike the gauge their propagation is limited by the speed of light; this issue is left to future work.

The main result about regularity is contained in the specific kinks and discontinuities discovered in both the power series and the numerical data, which are implied by our stationary solution. The construction of an explicit power series solution in r for a single Schwarzschild puncture can be repeated for a single puncture with Bowen-York linear momentum. Preliminary results indicate that the shift can acquire the constant leading term responsible for the motion of the punctures and that there are no new fundamental regularity issues. The power series ansatz matches nicely the numerical data for a Schwarzschild puncture. The fourth-order schemes (both centered and upwind) in use have been seen to be reasonably successful in this context, the lack of differentiability not withstanding [2,3]. Incidentally, the introduction of χ results in $O(r^2)$ terms and not $O(r^4)$ as expected, but this still results in significantly cleaner data than the log$r$ method. Perhaps most importantly, our analysis suggests a concrete remedy if the remaining numerical issues at the puncture create problems in simulations of black-hole binaries, namely, to resort to finite differencing that is expertly adapted to the discontinuities at hand.

Our results suggest several directions for future research directly relevant to the black-hole binary problem, such as perturbations of the stationary solutions (including constraint violating perturbations to check constraint stability of evolution systems), the clarification of numerical issues at the discontinuities, and the construction of initial data adapted to stationarity, e.g., of asymptotically cylindrical data. In the Schwarzschild case local properties of the stationary solution allow one to directly read off spacetime properties from a numerical solution, e.g., the puncture value of K determines the mass; an extension to two moving, spinning black holes would be very valuable in numerical evolutions.

[1] F. Pretorius, Phys. Rev. Lett. **95**, 121101 (2005).
[2] M. Campanelli, C. O. Lousto, P. Marronetti, and Y. Zlochower, Phys. Rev. Lett. **96**, 111101 (2006).
[3] J. G. Baker, J. Centrella, D.-I. Choi, M. Koppitz, and J. van Meter, Phys. Rev. Lett. **96**, 111102 (2006).
[4] B. Brügmann, W. Tichy, and N. Jansen, Phys. Rev. Lett. **92**, 211101 (2004).
[5] D. Brill and R. Lindquist, Phys. Rev. **131**, 471 (1963).
[6] S. Brandt and B. Brügmann, Phys. Rev. Lett. **78**, 3606 (1997).
[7] M. Alcubierre, W. Benger, B. Brügmann, G. Lanfermann, L. Nerger, E. Seidel, and R. Takahashi, Phys. Rev. Lett. **87**, 271103 (2001).
[8] B. Brügmann, Int. J. Mod. Phys. D **8**, 85 (1999).
[9] P. Diener *et al.*, Phys. Rev. Lett. **96**, 121101 (2006).
[10] M. Shibata and T. Nakamura, Phys. Rev. D **52**, 5428 (1995).
[11] T. W. Baumgarte and S. L. Shapiro, Phys. Rev. D **59**, 024007 (1998).
[12] M. Alcubierre, B. Brügmann, P. Diener, M. Koppitz, D. Pollney, E. Seidel, and R. Takahashi, Phys. Rev. D **67**, 084023 (2003).
[13] J. R. van Meter, J. G. Baker, M. Koppitz, and D.-I. Choi, Phys. Rev. D **73**, 124011 (2006).
[14] C. Gundlach and J. M. Martin-Garcia, Phys. Rev. D **74**, 024016 (2006).
[15] B. Brügmann, J. A. González, M. Hannam, S. Husa, U. Sperhake, and W. Tichy, arXiv:gr-qc/0610128.
[16] L. T. Buchman and J. M. Bardeen, Phys. Rev. D **72**, 124014 (2005).
[17] N. Ó Murchadha and K. Roszkowski, Classical Quantum Gravity **23**, 539 (2006).
[18] C. Bona and J. Massó, Phys. Rev. D **38**, 2419 (1988).
[19] G. B. Cook and M. A. Scheel, Phys. Rev. D **56**, 4775 (1997).
[20] F. Estabrook, H. Wahlquist, S. Christensen, B. DeWitt, L. Smarr, and E. Tsiang, Phys. Rev. D **7**, 2814 (1973).
[21] R. Beig and N. Ó Murchadha, Phys. Rev. D **57**, 4728 (1998).
[22] B. Reimann and B. Brügmann, Phys. Rev. D **69**, 044006 (2004).
[23] M. D. Hannam, C. R. Evans, G. B. Cook, and T. W. Baumgarte, Phys. Rev. D **68**, 064003 (2003).